ROYAL SOCIETY
OF CHEMISTRY

Check for updates

Modulation for efficiency and spectra of non-doped white organic light emitting diodes by combining an exciplex with an ultrathin phosphorescent emitter

Zemei Liu,[a] Bo Zhao, [ID] *[a] Yuan Gao,*[b] Haifeng Chen,[c] Bizheng Dong,[a] Yabo Xu,[a] Hua Wang, [ID] *[a] Bingshe Xu[a] and Wenlian Li[d]

Herein, structured non-doped white organic light-emitting diodes (WOLEDs) were designed by combining the emission of a blue exciplex and orange-red phosphorescent ultrathin layer. The device efficiency and spectra were modulated successfully by adjusting the thickness of the exciplex layer and ultrathin layer, respectively. Meanwhile, high efficiency with external quantum efficiency (EQE) ranging from 15% to 22%, power efficiency from 33 lm W^{-1} to 47 lm W^{-1} and warm white emission with correlated color temperature (CCT) from 1600 K to 2600 K were realized. The energy transfer process and emission mechanism is also discussed, and the results reveal that the efficient charge trapping and recombination contribute to the improvement of device efficiency and reduce the roll-off efficiency.

1. Introduction

White organic light emitting diodes (WOLEDs) exhibit huge application prospects in lighting fields due to their flexible lighting and natural plane light source. In general, a host–guest doped system is applied in the emitting layer (EML) structure of an OLED to reduce the exciton concentration quenching. Further, blue/orange or blue/green/red emitter-based multi-EMLs have to be used in WOLEDs to produce the white emission. Therefore, WOLEDs often consist of multi-EML host–guest-doped structures, and suffer from fabrication complexity, low repeatability, difficult concentration controllability and hard host material selectivity.[1–4] In order to overcome the above-mentioned disadvantages, the structured non-doped WOLED-based ultrathin layers were studied from the past literature.[5–8]

Besides the traditional-fluorescent,[9,10] phosphorescent[11,12] and thermally activated delayed fluorescence (TADF) emitter[13,14] based single molecular emission used in OLEDs, the bimolecular emission of an exciplex resulting from the

intermolecular charge transfer excited state, received significant attention since the discovery of triplet exciton reverse intersystem crossing (RISC) in 2012 by Adachi *et al.*[15] Subsequently, a series of high efficiency exciplex OLED-based blue, green and orange emissions were exploited by harvesting the triplet exciton through the RISC process.[16–19] Compared to the single molecular emission materials, exciplex OLEDs present some more advantages such as fluorescence emission with low cost, reduced power loss with low operating voltage and relative small roll-off efficiency with the wide exciton recombination zone. In particular, the low operating voltage benefitted from the barrier-free charge injection contributes to the improvement of the power efficiency and reduce power loss, which is an important parameter for WOLEDs. Therefore, it seems to be a promising method to combine the exciplex with the ultrathin layer to fabricate non-doped WOLEDs. Ying *et al.* employed an orange ultrathin phosphorescent emitter of Ir(tptpy)$_2$acac to insert into a different location of the blue co-doping exciplex host to achieve highly efficient non-doped WOLEDs.[20] Xu *et al.* fabricated efficient tandem non-doped WOLEDs by inserting blue and orange phosphorescent ultrathin emitters of FIrpic and PO-01, respectively, into the interface of a bi-layer exciplex.[21] Feng *et al.* utilized the energy transfer of a bi-layer exciplex by inserting an orange fluorescent ultrathin emitter of TBRb into the donor or acceptor to earn high efficiency non-doped WOLEDs.[22] Although some good results were realized through the combination of co-doping/bi-layer exciplex with ultrathin layer emitter, the influence on the efficiency and spectra of exciplex/ultrathin layer thickness is rarely researched in non-doped WOLEDs. Moreover, highly efficient and highly

[a]Key Laboratory of Interface Science and Engineering in Advanced Materials of Ministry of Education, Taiyuan University of Technology, Taiyuan 030024, China. E-mail: zhaobo01@tyut.edu.cn; wanghua001@tyut.edu.cn

[b]College of Economics and Management, Chongqing University of Arts and Sciences, Chongqing 402160, China. E-mail: yuangao@cqwu.edu.cn

[c]School of Electronic Information and Electrical Engineering, Chongqing University of Arts and Sciences, Chongqing 402160, China

[d]State Key Laboratory of Luminescence and Applications, Changchun Institute of Optics, Fine Mechanics and Physics, Chinese Academy of Sciences, Changchun 130033, China

color stable WOLED-based exciplexes and ultrathin layers still need to be investigated further.

In this work, we designed non-doped WOLEDs by combining the blue exciplex emission of *m*-bis(*N*-carbazolyl)benzene:(1,3,5-triazine-2,4,6-triyl) tris(benzene-3,1-diyl) tris(diphenylphosphineoxide) (**mCP:PO-T2T**) with orange-red ultrathin phosphorescent emitter iridium(III) bis(2-phenylquinoline) acetylacetonate (**Ir(pq)₂acac**) to achieve white light emission. The ultrathin phosphorescent layers were inserted into both sides of the exciplex layer, and the thickness of the ultrathin layer and exciplex layer was adjusted, respectively, to modulate the efficiency and spectra of WOLEDs. As a result, the efficiency and spectra are modulated successfully through the thickness with EQE ranging from 15% to 22%, power efficiency from 33 lm W^{-1} to 47 lm W^{-1} and the correlated color temperature (CCT) from 1600 K to 2600 K.

2. Experimental section

All the organic and inorganic materials used in this study were purchased from commercial sources and used without further purification. All OLEDs were fabricated on indium tin oxide (ITO)-coated glass substrates with a sheet resistance of 10 Ω sq^{-1}. The organic layers were deposited at a rate of 1.0 Å s^{-1}, and the inorganic layers of MoO_3 and LiF were deposited at a rate of 0.1 Å s^{-1}. An Al cathode was deposited in the end at a rate of 5.0 Å s^{-1} with a shadow mask, which defined a device area of 3×3 mm². The photoluminescence (PL) spectra were measured using a FluoroMax-4 fluorescence spectrometer (HORIBA Jobin Yvon). The UV-Vis absorption spectrum was recorded using a Hitachi U-3900 scanning spectrophotometer. The electroluminescence (EL) spectra were measured through a computer controlled PR-655 Spectra Scan spectrometer. The current–voltage–luminance curves were measured with Keithley 2400 power supply combined with a BM-7A luminance colorimeter. External quantum efficiency (EQE) was calculated from the current density–voltage–luminance curve and spectral data. Besides, all measurements were carried out at room temperature and under ambient conditions without any protective coatings.

3. Results and discussions

3.1 Photo-physical property of the exciplex

In this work, complementary colors of blue and orange-red are adopted to form white emission. **mCP** and **PO-T2T** are chosen as the electron donor and acceptor materials, respectively, to form the blue exciplex, and the phosphorescent emitter of **Ir(pq)₂acac** is selected as the orange-red emission ultrathin layer for WOLEDs. Fig. 1a shows the molecular structure of **mCP**, **PO-T2T** and **Ir(pq)₂acac**, and Fig. 1b exhibits the PL spectra of **mCP**, **PO-T2T**, **mCP:PO-T2T** mixed films (1 : 1) and absorption spectra of **Ir(pq)₂acac** emitters. The observed emission peak of 468 nm is from the **mCP:PO-T2T** mixed film that is different from the emission of the donor of **mCP** (365 nm) and acceptor of **PO-T2T** (381 nm), thus indicating the formation of the exciplex formation. Besides, the peak value of 2.64 eV is similar to the energy gap between the highest occupied molecular orbital (HOMO) of **mCP** (6.1 eV) and lowest unoccupied molecular orbital (LUMO) of **PO-T2T** (3.5 eV), which also demonstrates the formation of the exciplex between **mCP** and **PO-T2T**. The OLED-based **mCP:PO-T2T** exciplex also had been reported for highly efficient blue emission, which could reach a high EQE of 8% due to the long-lifetime TADF emission.[23] The high efficiency of the exciplex could also provide an efficient blue emission in our WOLEDs. The large overlap between the absorption spectra of the **Ir(pq)₂acac** phosphorescent emitter and the PL spectrum of **mCP:PO-T2T** exciplex could be observed, and indicate that a high Förster energy transfer efficiency from the exciplex to **Ir(pq)₂acac** could occur.[24]

3.2 Doped WOLED-based exciplex host

Based on the above-mentioned photo-physical discussion, we first designed a doped WOLED with the device structure of ITO/MoO_3 (3 nm)/**mCP** (30 nm)/**mCP:PO-T2T** (1 : 1): x wt% **Ir(pq)₂-acac** (15 nm)/**PO-T2T** (40 nm)/LiF (1 nm)/Al, $x = 0.3$ and 0.6, and the corresponding WOLED is defined as $W_{0.3}$ and $W_{0.6}$, respectively. **mCP:PO-T2T** (1 : 1): x wt% **Ir(pq)₂acac** is the EML with exciplex as the host to sensitize **Ir(pq)₂acac**, while **mCP** and **PO-T2T** are the hole transport layer (HTL) and electron
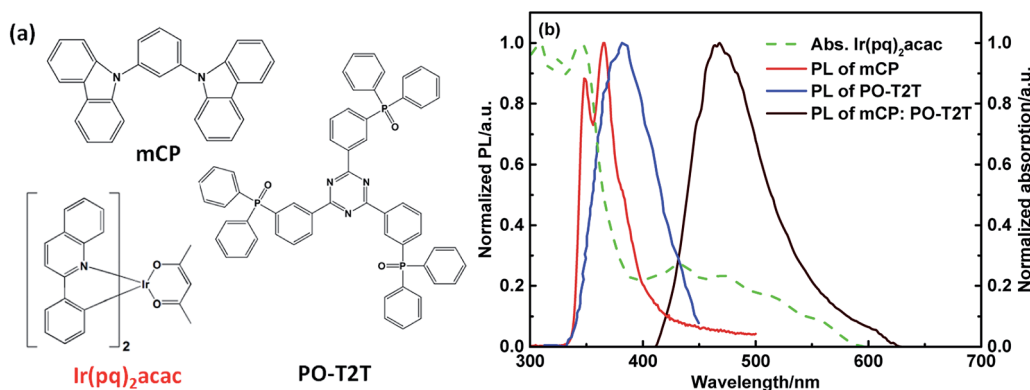

Fig. 1 (a) The molecular structure of **mCP**, **PO-T2T** and **Ir(pq)₂acac**. (b) The absorption spectrum of **Ir(pq)₂acac**, and PL spectra of **mCP**, **PO-T2T** and **mCP:PO-T2T** mixed film.

transport layer (ETL), respectively. The current density, luminance and efficiency characteristic curves are shown in Fig. 2. The WOLED achieves low operation voltages of 3.86 V and 3.71 V under 1000 cd m^{-2} with $W_{0.3}$ and $W_{0.6}$, respectively, and a high luminance of ~10 000 cd m^{-2}. The low operation voltage is a benefit from the barrier-free charge injection from the transport layer to EML due to the same organic materials of HTL/donor and ETL/acceptor. Besides, the charge recombination between the HOMO of **mCP** and the LUMO of **PO-T2T** also contributes to the formation of exciplex to reduce the operational voltage.

The maximum current efficiency (CE), power efficiency (PE) and EQE of $W_{0.3}$ are 35.4 cd A^{-1}, 39.1 lm W^{-1} and 16.9%, respectively, while the higher efficiency of 39.2 cd A^{-1}, 43.2 lm W^{-1} and 18.5% are realized with a higher concentration in $W_{0.6}$. However, the roll-off efficiency from maximum EQE to EQE at 1000 cd m^{-2} is significant. The EQE of $W_{0.3}$ at 1000 cd m^{-2} is 9.0% with the roll-off ratio at 46.7%, and a similar situation occurs in $W_{0.6}$; the EQE at 1000 cd m^{-2} is 12.1% and the roll-off ratio is 34.8%. The large roll-off efficiency may arise from high triplet exciton concentration, which results in the significant triplet–triplet annihilation (TTA) and singlet-triplet annihilation (STA). The Dexter energy transfer process from **mCP:PO-T2T** to **Ir(pq)$_2$acac** and direct charge trapping recombination in **Ir(pq)$_2$acac** is difficult to happen due to the low doping concentration; thus, the emission of **Ir(pq)$_2$acac** is from the Förster energy transfer between the singlet energy level of **mCP:PO-T2T** and **Ir(pq)$_2$acac**. Therefore, the RISC in **mCP:PO-T2T** plays a crucial function and the high RISC efficiency can reduce triplet concentration efficiently. Hence, the serious roll-off efficiency could be considered as high triplet concentration with low RISC efficiency in the **mCP:PO-T2T** exciplex.[23]

The EL spectra of $W_{0.3}$ and $W_{0.6}$ are shown in Fig. 3. The spectra exhibit white emission with two emission peaks of blue emission at 480 nm and orange-red emission at 590 nm, which stem from the **mCP:PO-T2T** exciplex host and **Ir(pq)$_2$acac**, respectively. We also did the higher doping concentration; however, the too weak exciplex blue emission impedes the

formation of white light emission. Further, as the concentration increases from 0.3 wt% to 0.6 wt%, the exciplex blue emission intensity reduces, and demonstrates efficient energy transfer from the exciplex host to the dopant. The stability Commission
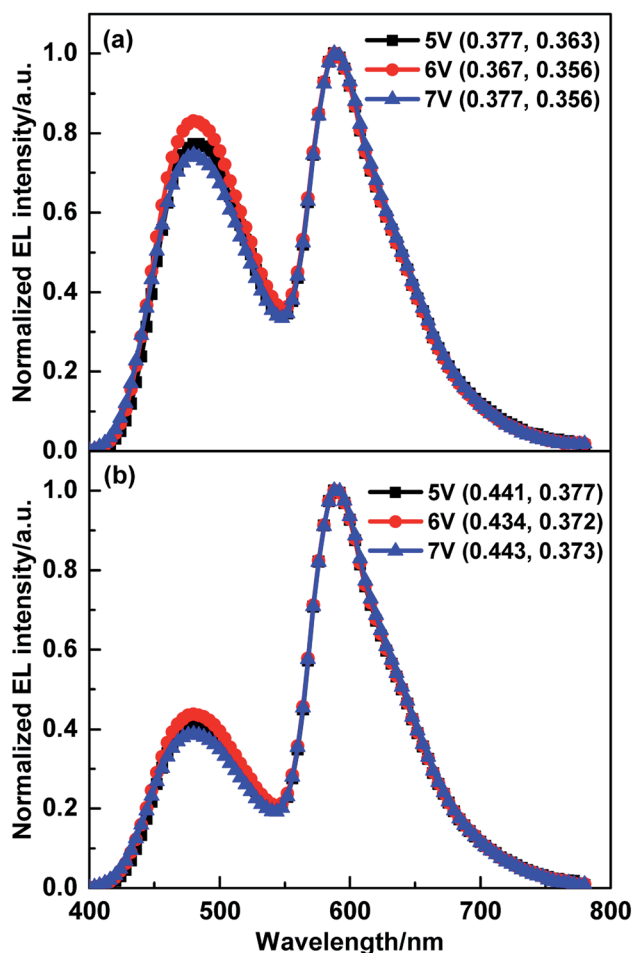

Fig. 3 The EL spectra of doped structural WOLED. (a) 0.3 wt%. (b) 0.6 wt%.
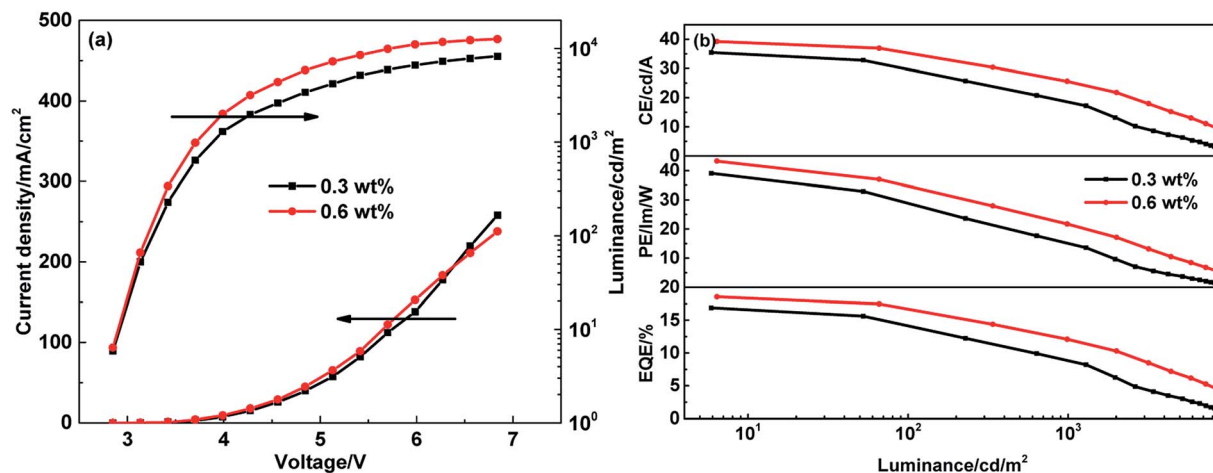

Fig. 2 The EL performance of doped structural WOLED. (a) Current density–voltage–luminance curves. (b) CE, PE and EQE–luminance curves.
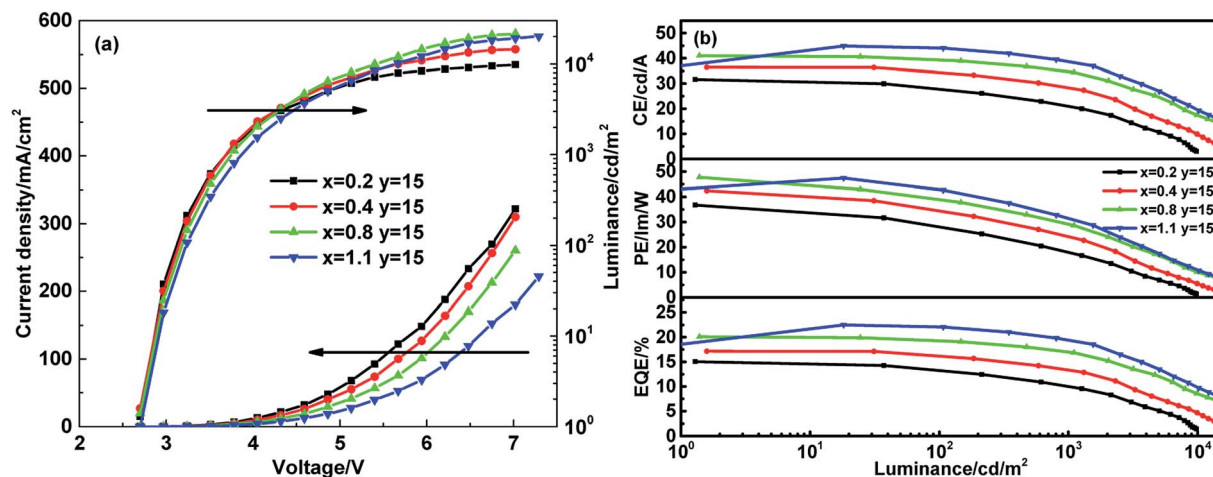
Fig. 4 The EL performance of non-doped structural WOLED with different-thickness ultrathin layers. (a) Current density–voltage–luminance curves. (b) CE, PE and EQE–luminance curves.

Internationale de l'Eclairage (CIE) coordination of (0.367, 0.356) and (0.434, 0.372) at 6 V are also achieved in $W_{0.3}$ and $W_{0.6}$, respectively. Hence, the low operation voltage, high efficiency and high color stability WOLED with doped structure of the **mCP:PO-T2T** exciplex as the host and **Ir(pq)$_2$acac** as the dopant are realized.

3.3 Non-doped WOLED-based exciplex and ultrathin layer

The doped structural WOLED with a low concentration of **Ir(pq)$_2$acac** in exciplex host of 0.3 wt% and 0.6 wt% suffered from hard concentration precision control and low repeatability. Thus, in this section, we designed the structured non-
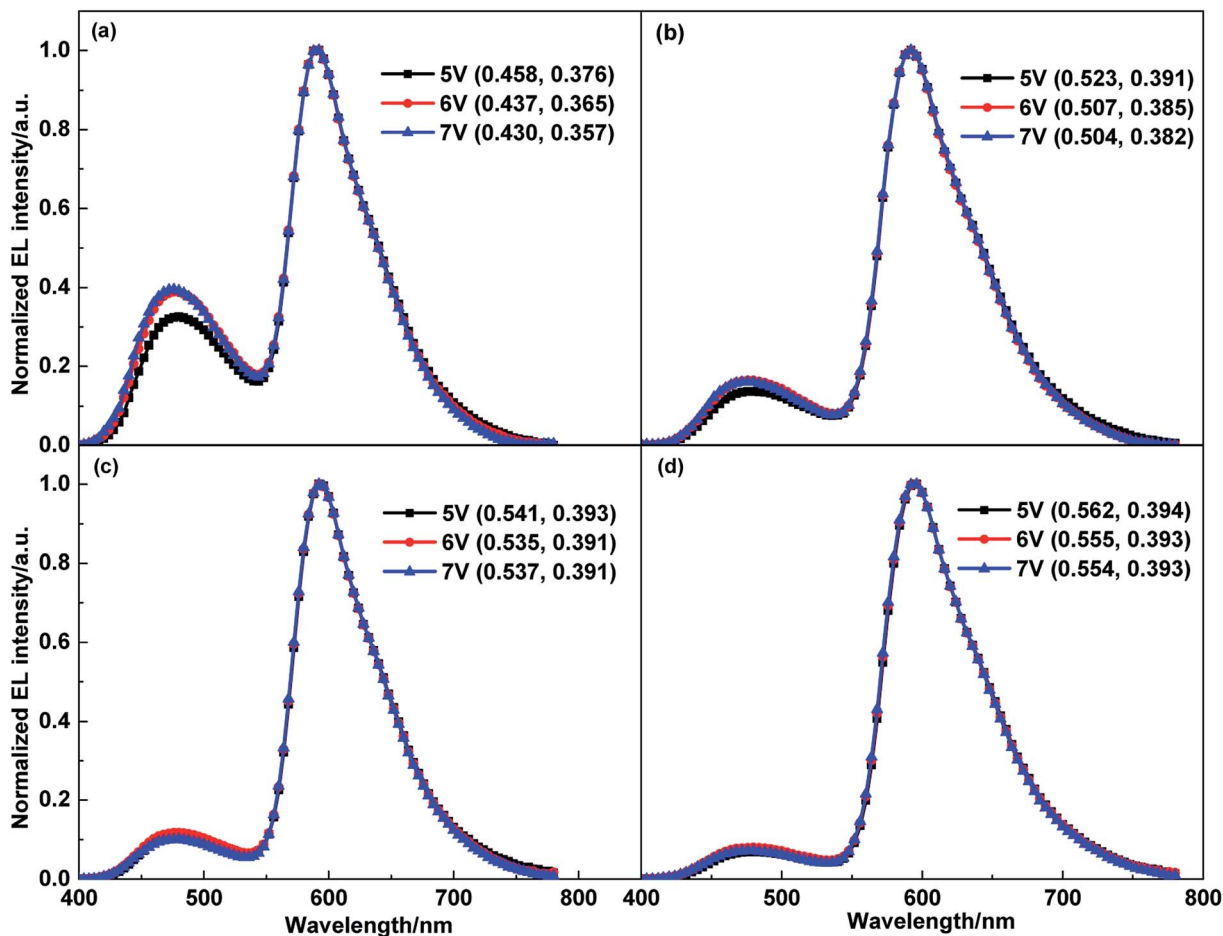

Fig. 5 The EL spectra of structured non-doped WOLED with different ultrathin layer thickness. (a) $x = 0.2$. (b) $x = 0.4$. (c) $x = 0.8$. (d) $x = 1.1$.

doped WOLED by combining **mCP:PO-T2T** exciplex with ultrathin layer **Ir(pq)₂acac**. Further, **Ir(pq)₂acac** ultrathin layers were inserted into both sides of exciplex EML to construct the non-doped WOLED. The device structure of ITO/MoO$_3$ (3 nm)/**mCP** (30 nm)/**Ir(pq)₂acac** (x nm)/**mCP:PO-T2T** (1 : 1) (y nm)/**Ir(pq)₂-acac** (x nm)/**PO-T2T** (40 nm)/LiF (1 nm)/Al was adopted. Here, x = 0.2, 0.4, 0.8, 1.1 and y = 15, and the corresponding WOLED is defined as W$_{0.2/15}$, W$_{0.4/15}$, W$_{0.8/15}$ and W$_{1.1/15}$, respectively. The **mCP:PO-T2T** exciplex EML provides the blue emission, and ultrathin layer of **Ir(pq)₂acac** acts as the orange-red emission to form the white emission. Firstly, we fix the exciplex EML thickness as 15 nm, which is same as the thickness of EML in doped WOLED, and the **Ir(pq)₂acac** ultrathin layer is adjusted with four thickness values from 0.2 nm to 1.1 nm.

The current density, luminance and efficiency curves are shown in Fig. 4. Similar to the aforementioned doped WOLED, the non-doped WOLED also achieves a low operation voltage in the range of 3.6–3.8 V at 1000 cd m^{-2} and high luminance of ~10 000 cd m^{-2}. Although the exciplex layer is separated from the transport layer by inserting the **Ir(pq)₂acac** layer, the ultrathin thickness from 0.2 nm to 1.1 nm makes the **Ir(pq)₂acac** film discontinuous, which also ensures the efficient charge injection. Therefore, the barrier-free charge injection from transport layer to EML is also suitable for the non-doped

WOLED, which results in low operation voltage. However, the reduced current density with increased thickness of ultrathin layer demonstrates the efficient charge trapping by the **Ir(pq)₂acac** emitter. Therefore, we consider that the orange-red emission is mainly from the direct charge trapping recombination by the **Ir(pq)₂acac** molecule rather than the energy transfer from the **mCP:PO-T2T** exciplex.[25,26] The maximum CEs, PEs and EQEs of W$_{0.2/15}$/W$_{0.4/15}$/W$_{0.8/15}$/W$_{1.1/15}$ shown in Fig. 4b are 31.6/36.5/41.1/44.9 cd A^{-1}, 36.8/42.4/47.7/47.4 lm W^{-1} and 15.1/17.1/20.1/22.5%, respectively. The peak PE ~47 lm W^{-1} satisfies the efficiency requirement of PE > 40 lm W^{-1} for commercial applications of WOLED. The EQE of ~20% also reaches the upper limit in phosphorescent WOLED without the optically coupled output structure. While the relatively small roll-off efficiency from maximum EQE to EQE under 1000 cd m^{-2} with roll-off ratios at 32.9%, 21.6%, 15.2% and 13.4% are also realized, respectively, it is much lower than the doped WOLED with the roll-off ratios of 46.7% and 34.8%. Furthermore, we found that the roll-off ratio decreases from 32.9% to 13.4% with the increased thickness of ultrathin layer. We consider that the direct charge trapping of the **Ir(pq)₂acac** emitter to carrier plays the important role and decreases the carrier injection, recombination and exciton formation in the **mCP:PO-T2T** exciplex. Therefore, the relative low singlet and
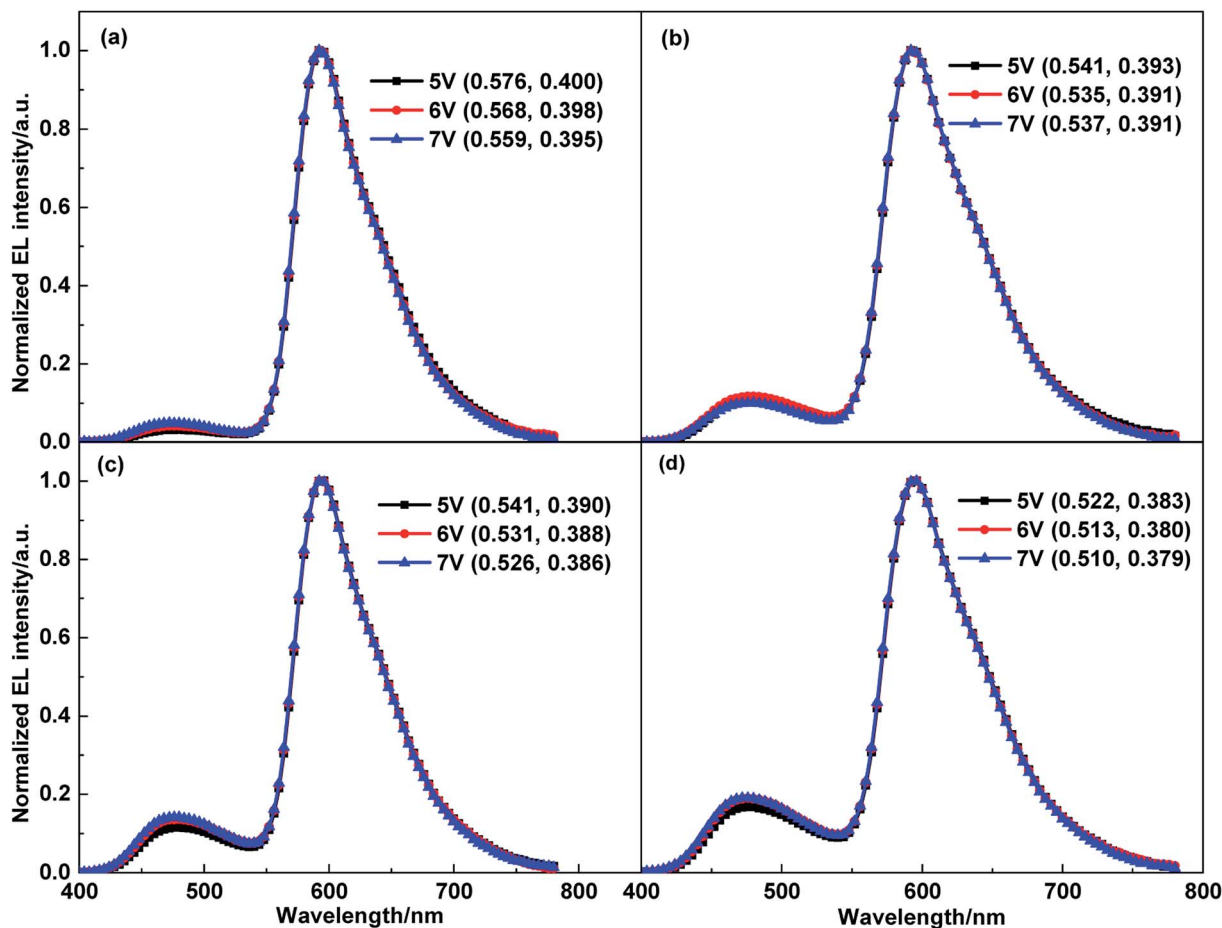

Fig. 6 The EL spectra of structured non-doped WOLED with different-thickness exciplex layers. (a) y = 10. (b) y = 15. (c) y = 20. (d) y = 25.
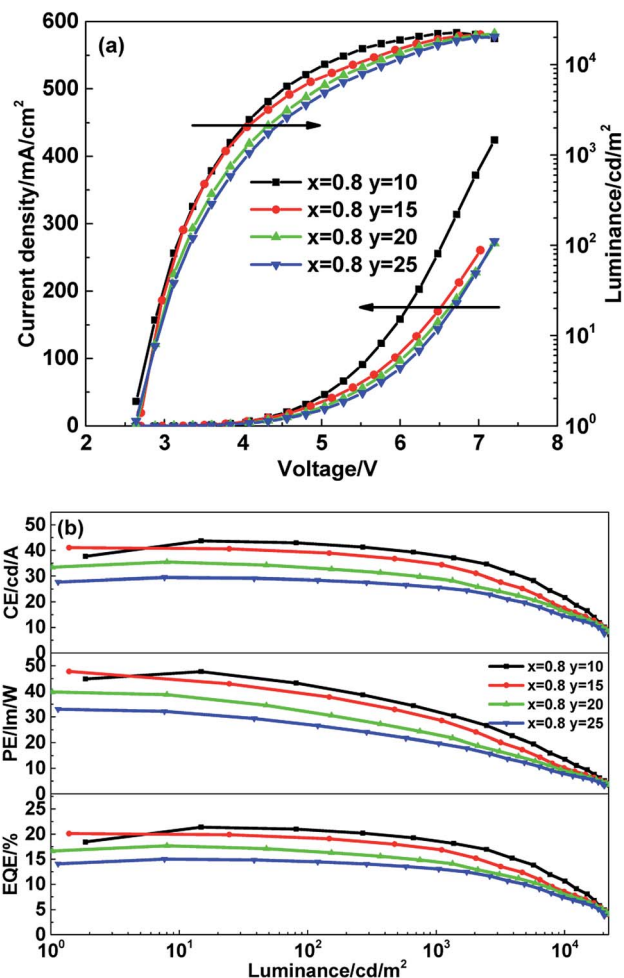
Fig. 7 The EL performance of structured non-doped WOLED with different-thickness exciplex layers. (a) Current density–voltage–luminance curves. (b) CE, PE and EQE–luminance curves.

triplet exciton concentration in exciplex EML contributes to the reduce of the roll-off efficiency compared to the doped structural WOLED. This means that the roll-off efficiency is mainly derived from the high exciplex exciton concentration quenching rather than the **Ir(pq)₂acac** exciton concentration.

The thicker **Ir(pq)₂acac** layer could capture more carriers and improve the orange-red emission intensity, and the EL spectra from $W_{0.2/15}$ to $W_{1.1/15}$ are displayed in Fig. 5. All four WOLEDs exhibit pure blue exciplex and orange-red ultrathin layer emission, and just as we expected the blue emission intensity reduces with the enhanced thickness of ultrathin layers. The warm white emission WOLEDs with CIE coordinates of (0.437, 0.365), (0.507, 0.385), (0.535, 0.391) and (0.555, 0.393) at 6 V are realized, and the CCTs ranging from 1600 K to 2600 K are closed for commercial application of warm white light (∼2800 K). As a result, the white emission spectra could be modulated by changing the ultrathin layer thickness.

Besides the ultrathin layer thickness could adjust the white emission spectra, and we considered that the blue exciplex EML thickness could also be optimized to achieve the modulation for white emission spectra. Thus, in this section, we discuss the same non-doped WOLED structure by fixing the ultrathin layer thickness at 0.8 nm, and exciplex EML thickness at 10, 15, 20 and 25 nm, correspondingly, which is $x = 0.8$ and $y = 10$, 15, 20, 25, and the corresponding WOLED is defined for $W_{0.8/10}$, $W_{0.8/15}$, $W_{0.8/20}$ and $W_{0.8/25}$, respectively. The ultrathin layer thickness of 0.8 nm is adopted due to the high EQE (>20%) and stable white emission spectra in $W_{0.8/15}$. The EL spectra of WOLED with different exciplex layer thicknesses are shown in Fig. 6. We can see that the blue emission intensity enhances as the exciplex layer thickness increases, which indicates that more charges recombine in the exciplex EML. Meanwhile, the stable white emission spectra are also obtained from $W_{0.8/10}$ to $W_{0.8/25}$ with CIE coordinates of (0.568, 0.398), (0.535, 0.391), (0.531, 0.388) and (0.513, 0.380) at 6 V.

The current density, luminance and efficiency performance curves are exhibited in Fig. 7. It is impressive that all four WOLEDs maintain a low turn-on voltage of ∼2.6 V in spite of the exciplex EML thickness ranging from 10 nm to 25 nm, which means that the charge injection barrier from the transport layer to EML is responsible for the turn-on voltage rather than the EML thickness. Further, a low operation voltage at 1000 cd m⁻² for the four WOLEDs is also achieved within the range of 3.7–4.0 V. As discussed above, the barrier-free injection of electrons and holes from the transport layer to EML contribute to the low

Table 1   A summary of the performance of all WOLEDs in this paper

Device	Voltage (V) (10^3 cd m⁻²)	CE (cd A⁻¹) (max/10^3 cd m⁻²)	PE (lm W⁻¹) (max/10^3 cd m⁻²)	EQE (%) (max/10^3 cd m⁻²)	Roll-off ratio[a]	CIE (6 V)	CCT (K) (6 V)
$W_{0.3}$	3.86	35.4/18.9	39.1/15.4	16.9/9.0	46.7%	(0.367, 0.356)	4240
$W_{0.6}$	3.71	39.2/25.6	43.2/21.7	18.5/12.1	34.8%	(0.434, 0.372)	2775
$W_{0.2/15}$	3.66	31.6/21.3	36.8/18.2	15.1/10.1	32.9%	(0.437, 0.365)	2653
$W_{0.4/15}$	3.67	36.5/28.6	42.4/24.6	17.1/13.4	21.6%	(0.507, 0.385)	1991
$W_{0.8/15}$	3.73	41.1/34.8	47.7/29.4	20.1/17.0	15.2%	(0.535, 0.391)	1802
$W_{1.1/15}$	3.84	44.9/38.9	47.4/31.8	22.5/19.5	13.4%	(0.555, 0.393)	1678
$W_{0.8/10}$	3.70	43.8/38.3	47.7/32.4	21.4/18.7	12.5%	(0.568, 0.398)	1625
$W_{0.8/15}$	3.73	41.1/34.8	47.7/29.4	20.1/17.0	15.2%	(0.535, 0.391)	1802
$W_{0.8/20}$	3.93	35.5/29.2	39.7/23.2	17.7/14.5	17.9%	(0.531, 0.388)	1811
$W_{0.8/25}$	4.01	29.5/25.7	33.0/19.9	15.0/13.1	12.9%	(0.513, 0.380)	1905

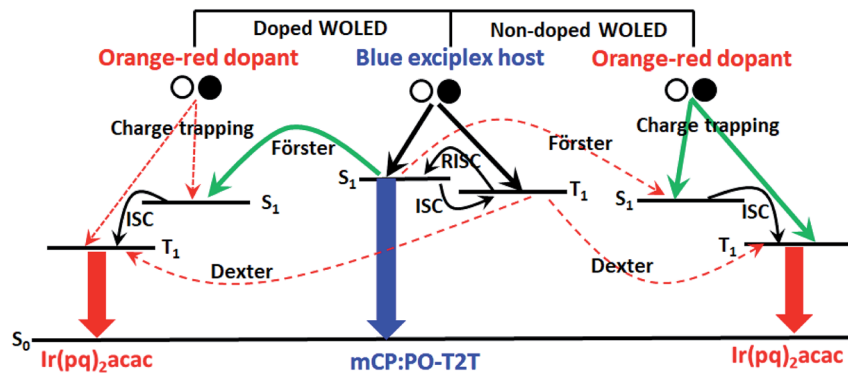[a] The efficiency roll-off ratio from maximum EQE to EQE at 1000 cd m⁻².

Fig. 8 The schematic of the energy transfer process and emission mechanism in doped and non-doped WOLEDs.

turn-on voltage and operation voltage. The efficiency curves of $W_{0.8/10}/W_{0.8/15}/W_{0.8/20}/W_{0.8/25}$ shown in Fig. 7b have maximum CEs, PEs and EQEs with 43.8/41.1/35.5/29.5 cd A^{-1}, 47.7/47.7/39.7/33.0 lm W^{-1} and 21.4/20.1/17.7/15.0%, respectively. Even at a high luminance of 1000 cd m^{-2}, EQEs still maintain a high value and the roll-off ratios are 12.5%, 15.2%, 17.9% and 12.9%, respectively. Hence, the structured non-doped WOLED discussed here either with different ultrathin layer thickness or different exciplex layer thickness have lower roll-off efficiency than the doped structural WOLED. The direct trapping recombination emission of **Ir(pq)₂acac** molecules in the structured non-doped WOLED reduces the vast exciton formation on the **mCP:PO-T2T** exciplex and suppresses the energy transfer from the exciplex to **Ir(pq)₂acac**. Therefore, the reduction of the RISC process in the **mCP:PO-T2T** exciplex helps to weaken TTA and STA, which results in lower roll-off efficiency in the non-doped WOLED than in the doped WOLED. The performances of all WOLEDs in this paper are listed in Table 1.

In order to further clarify the charge trapping, transport and recombination process in doped and non-doped WOLEDs, we depict the emission schematic in Fig. 8. In the doped structural WOLED, electrons and holes are injected into EML and recombined on the exciplex host to form exciplex singlet and triplet excitons. The direct charge trapping of **Ir(pq)₂acac** and Dexter energy transfer from the exciplex triplet state level to the **Ir(pq)₂acac** triplet state level could be ignored due to the low doping concentration of 0.3 wt% and 0.6 wt%.[27] Therefore, the emission of **Ir(pq)₂acac** comes from the long range Förster resonance energy transfer between the singlet state level of the exciplex host and dopant, which could be confirmed from almost the same current density curves of different concentrations, as shown in Fig. 2a. On the other hand, the singlet and triplet excitons of the exciplex host could convert each other through the ISC/RISC process; however, this could also lead to serious roll-off efficiency because of the long excitons lifetime and high excitons concentration.[28,29] However, in the non-doped WOLED, the ultrathin layer **Ir(pq)₂acac** in the interface of EML and transport layer could trap the charge efficiently, and the current density decreases with an increase in the thickness of the ultrathin layer, thus demonstrating the direct charge trapping effect. Therefore, the emission of **Ir(pq)₂acac** derives from

the direct charge trapping recombination. Due to the charge trapping impact, the charge recombination on the exciplex host reduces and makes the exciplex exciton concentration decrease, which results in the reduced roll-off efficiency in non-doped WOLED compared to the doped WOLED. Therefore, in the structured non-doped WOLED, the white emission is formed from the charge recombination on blue exciplex and direct charge trapping recombination on the orange-red **Ir(pq)₂acac** ultrathin layer.

4. Conclusion

In summary, doped and structured non-doped WOLEDs through the combination of a blue exciplex and orange-red ultrathin layer are designed successfully. The reduced roll-off efficiency is obtained in the non-doped WOLED in comparison to the doped structure. The modulation for device efficiency and spectra in the non-doped WOLED are also realized through the adjustment of the exciplex EML and ultrathin layer thickness. As a result, the EQE ranging from 15% to 22%, power efficiency from 33 lm W^{-1} to 47 lm W^{-1} and CCT from 1600 K to 2600 K are achieved, and the efficient charge trapping and recombination contribute to the improvement of the device efficiency and reduce the roll-off efficiency. We believe that the combination of an exciplex and ultrathin layer would be a promising method to simplify the WOLED structure and improve device performance.

Conflicts of interest

There are no conflicts of interest to declare.

Acknowledgements

Notes and references

1 J. Kido, K. Hongawa, K. Okuyama and K. Nagai, *Appl. Phys. Lett.*, 1994, **64**, 815–817.

2 B. Zhao, Z. Su, W. Li, B. Chu, F. Jin, X. Yan, F. Zhang, D. Fan, T. Zhang, Y. Gao and J. Wang, *Appl. Phys. Lett.*, 2012, **101**, 053310.

3 N. Sun, Q. Wang, Y. B. Zhao, Y. H. Chen, D. Z. Yang, F. C. Zhao, J. S. Chen and D. G. Ma, *Adv. Mater.*, 2014, **26**, 1617–1621.

4 J. Nishide, H. Nakanotani, Y. Hiraga and C. Adachi, *Appl. Phys. Lett.*, 2014, **104**, 233304.

5 C. Hakim, F. Alexis, F. Sébastien, C. Sébastien, C. Marie-Claude, A. Dominique, S. Alain and G. Bernard, *Appl. Phys. Lett.*, 2006, **89**, 183513.

6 Y. M. Wang, F. Teng, Z. Xu, Y. B. Hou, S. Y. Yang and X. R. Xu, *Mater. Chem. Phys.*, 2005, **92**, 291–294.

7 Y. B. Zhao, J. S. Chen and D. G. Ma, *ACS Appl. Mater. Interfaces*, 2013, **5**, 965–971.

8 B. Zhao, H. Zhang, Z. Wang, Y. Miao, Z. Wang, J. Li, H. Wang, Y. Hao and W. Li, *J. Mater. Chem. C*, 2018, **6**, 4250–4256.

9 C. W. Tang and S. A. VanSlyke, *Appl. Phys. Lett.*, 1987, **51**, 913–915.

10 B. Zhao, Y. Miao, Z. Wang, K. Wang, H. Wang, Y. Hao, B. Xu and W. Li, *Nanophotonics*, 2016, **6**, 1133–1140.

11 M. A. Baldo, D. F. O'Brien, Y. You, A. Shoustikov, S. Sibley, M. E. Thompson and S. R. Forrest, *Nature*, 1998, **395**, 151–154.

12 B. Tong, Q. Mei, R. Tian, M. Yang, Q. Hua, Y. Shi and S. Ye, *RSC Adv.*, 2016, **6**, 34970–34976.

13 H. Uoyama, K. Goushi, K. Shizu, H. Nomura and C. Adachi, *Nature*, 2012, **492**, 234–238.

14 J. Li, R. Zhang, Z. Q. Wang, B. Zhao, J. J. Xie, F. Zhang, H. Wang and K. P. Guo, *Adv. Opt. Mater.*, 2018, **6**, 1701256.

15 K. Goushi, K. Yoshida, K. Sato and C. Adachi, *Nat. Photonics*, 2012, **6**, 253–258.

16 T. Y. Zhang, B. Zhao, B. Chu, W. L. Li, Z. S. Su, X. W. Yan, C. Y. Liu, H. R. Wu, F. M. Jin and Y. Gao, *Org. Electron.*, 2015, **25**, 6–11.

17 W. Liu, J. X. Chen, C. J. Zheng, K. Wang, D. Y. Chen, F. Li, Y. P. Dong, C. S. Lee, X. M. Ou and X. H. Zhang, *Adv. Funct. Mater.*, 2016, **26**, 2002–2008.

18 Q. T. Siddiqui, A. A. Awasthi, P. Bhui, P. Parab, M. Muneer, S. Bose and N. Agarwal, *RSC Adv.*, 2019, **9**, 40248–40254.

19 M. Chapran, P. Pander, M. Vasylieva, G. W. Salyga, J. Ulanski, F. B. Dias and P. Data, *ACS Appl. Mater. Interfaces*, 2019, **11**, 13460–13471.

20 S. Ying, J. Yao, Y. Chen and D. Ma, *J. Mater. Chem. C*, 2018, **6**, 7070–7076.

21 T. Xu, J. G. Zhou, M. K. Fung and H. Meng, *Org. Electron.*, 2018, **63**, 369–375.

22 D. Feng, D. Dong, L. Lian, H. Wang and G. He, *Org. Electron.*, 2018, **56**, 216–220.

23 W. Y. Hung, G. C. Fang, S. W. Lin, S. H. Cheng, K. T. Wong, T. Y. Kuo and P. T. Chou, *Sci. Rep.*, 2014, **4**, 5161.

24 Z. Q. Wang, C. Wang, H. Zhang, Z. M. Liu, B. Zhao and W. L. Li, *Org. Electron.*, 2019, **66**, 227–241.

25 C. Weichsel, L. Burtone, S. Reineke, S. I. Hintschich, M. C. Gather, K. Leo and B. Lüssem, *Phys. Rev. B: Condens. Matter Mater. Phys.*, 2012, **86**, 075204.

26 L. Zhu, Z. Wu, J. Chen and D. Ma, *J. Mater. Chem. C*, 2015, **3**, 3304–3310.

27 J. H. Lee, S. Lee, S. J. Yoo, K. H. Kim and J. J. Kim, *Adv. Funct. Mater.*, 2014, **24**, 4681–4688.

28 J. H. Lee, S. H. Cheng, S. J. Yoo, H. Shin, J. H. Chang, C. I. Wu, K. T. Wong and J. J. Kim, *Adv. Funct. Mater.*, 2014, **25**, 361–366.

29 J. W. Sun, K. H. Kim, C. K. Moon, J. H. Lee and J. J. Kim, *ACS Appl. Mater. Interfaces*, 2016, **8**, 9806–9810.